



# Low Overhead and High Stability Radiation-Hardened Latch for Double/Triple Node Upsets

Zhengfeng Huang<sup>1</sup> · Hao Wang<sup>1</sup> · Dongxing Ma<sup>1</sup> · Huaguo Liang<sup>1</sup> · Yiming Ouyang<sup>2</sup> · Aibin Yan<sup>3</sup>

Received: 31 August 2022 / Accepted: 8 April 2023 / Published online: 9 May 2023  
© The Author(s), under exclusive licence to Springer Science+Business Media, LLC, part of Springer Nature 2023

## Abstract

To tolerate Double Nodes Upset (DNU) and Triple Nodes Upset (TNU), we propose the DNU Tolerant Latch (DNUL) and TNU Tolerant Latch (TNUL) with low overhead and high stability. Both DNUL and TNUL are composed of the looped Input-Split C-Elements (ISCs) and the C-Elements (CEs) at the output level. Based on the robust blocking ability of the ISCs, the simultaneous upset of all inputs of the CE can be blocked. DNUL and TNUL have low overhead with fewer transistors by utilizing the clock-gating and high-speed path technique. Exhaustive HSPICE simulation shows that, in contrast to previous DNU tolerant latches, DNUL is optimal in terms of delay, power consumption and product of delay and power (PDP), but is suboptimal in terms of area overhead. Compared with all alternative structures, TNUL is the best in terms of delay and PDP. Compared to other TNU tolerant latches, TNUL achieves a suboptimal power consumption and area overhead. Variation analysis shows that DNUL and TNUL are insensitive to variations of process, voltage and temperature (PVT).

**Keywords** Single Event Upset · Double Nodes Upset · Triple Nodes Upset · C-Element · Radiation hardened

---

Responsible Editor: A. Orailoglu

✉ Aibin Yan  
abyan@mail.ustc.edu.cn  
Zhengfeng Huang  
huangzhengfeng@139.com  
Hao Wang  
2190670786@qq.com  
Dongxing Ma  
1015329151@qq.com  
Huaguo Liang  
huagulg@hfut.edu.cn  
Yiming Ouyang  
oyymbox@163.com

<sup>1</sup> School of Microelectronics, Hefei University of Technology, Hefei 230601, China

<sup>2</sup> School of Computer Science and Information Engineering, Hefei University of Technology, Hefei 230601, China

<sup>3</sup> School of Computer Science and Technology, Anhui University, Hefei 230601, China

## 1 Introduction

With the scaling of the integrated circuits, the feature size of transistors has entered the nano-scale. The supply voltage and node capacitance are decreasing, causing a constant decrease in the critical charge of the internal nodes [14]. When the energetic particles hit the sensitive regions of the device, charges are deposited on their trajectory of movement. These deposited charges will be collected by source/drain during drift and diffusion. When the collected charge exceeds the critical charge of the node, the logic value of the node will be upset [9]. When the effect occurs in sequential logic, such as latches and flip-flops, it is called Single Event Upset (SEU). If the SEU occurs and causes the logic value of a single node of the storage module to upset, it is called a Single Node Upset (SNU). Due to the decrease in feature sizes, the distance between the internal nodes continually decreases. Because of the effect of charge sharing, the deposited charges may be simultaneously collected by two or more internal nodes [7, 24]. This causes the Double Nodes Upset (DNU) or Multiple Nodes Upset (MNU) [21]. In particular, the aerospace is littered with high energy particles such as protons, neutrons,  $\alpha$  particles and  $\gamma$  Rays, which increases the probability of SNU and MNU for space applications [3, 6]. Prior research shows that DNU and MNU

have become the most dominant factors inducing soft errors in sequential elements [10]. Radiation Hardened By Design (RHBD) is suitable for mitigating SNU/MNU and can effectively harden circuits to provide high reliability. In addition, there are device-level and system-level hardened methods, such as Radiation Hardened By Process (RHBP) and Error Correction Codes (ECC) [5].

In this paper, we propose a low overhead DNU tolerant latch (DNUL). Based on the robust blocking ability of Input-Split C-Elements (ISCs) [11], six ISCs are connected into a large subtle feedback loop. And specific three internal nodes feed the Triple-input C-Element (TCE) to provide the output. DNUL achieves complete tolerance of DNU. We also propose a low overhead TNU tolerant latch (TNUL), as an extension of DNUL. The number of ISCs in the feedback loop is increased to eight. And specific four internal nodes feed the two-level CEs to provide the output. TNUL achieves complete tolerance of DNU. The proposed latches utilize a high-speed path technique to reduce the propagation delay. The introduction of clocked ISCs and clocked C-Elements can effectively reduce the power consumption. Extensive HSPICE simulation shows that the proposed latches achieve advantages in terms of delay, power consumption, PDP and area overhead. Variation analysis shows that the proposed latches are insensitive to process, voltage and temperature (PVT) variations.

The rest of the paper is organized as follows: Section 2 describes the previous hardened latches; Section 3 introduces the circuit schematic, working principle and fault-tolerant principle of DNUL and TNUL; Section 4 evaluates the hardened performance, overhead and sensitivity to variation; Section 5 summarizes this paper.

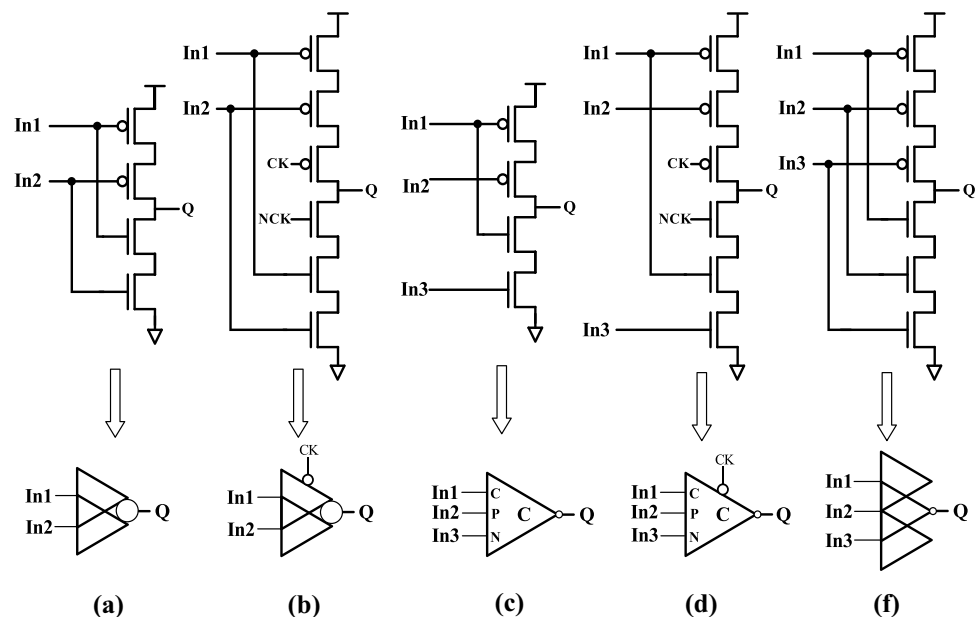
## 2 The Previous Hardened Latch Designs

Figure 1 shows the basic elements which have been commonly used in previous hardened latches. Figure 1a is the C-Element (CE) [13]. Figure 1b is the clocked CE. Figure 1c is the ISC, ISC is the abbreviation of Input-Split C-Element. Because compared with the C-Element, ISC is equivalent to separating one input of C-Element into two inputs. Therefore, it is defined as Input-Split C-Element (ISC) [11]. Figure 1d is the clocked ISC. Figure 1e is the TCE. As we can see from Fig. 1a, when two inputs of the CE are the same, the output is reverse to the input. The output temporarily holds the previous logic value when the CE has two different inputs. In the same way, the TCE has the same property, i.e., the output temporarily holds the previous logic value when the inputs are different.

Under the premise that the number of transistors is the same as for CE, the ISC not only has the ability like the CE to block SNU, but also has the effective ability to block DNU. When the logic values of the three inputs are the same, the ISC works normally. When the inputs CPN = 000, Q = 1. After DNU occurs at the inputs of ISC, the logic value of the CPN may be upset to 110, 101 or 011. According to the structure of ISC, Q upsets to 0 if and only if the CPN is upset to 101. Similarly, when CPN = 111, Q upsets if and only if CPN is upset to 001. In addition, if CPN is upset in either case, Q will be in the “hold” state. So, the DNU tolerance rate of ISC is 2/3. Next we will briefly introduce the previous hardened latches.

DONUT [4] in Fig. 2a is a DNU tolerant latch. DONUT can be seen as a combination of 4 Dual Interlocked storage Cells (DICE) [2], and uses the SNU tolerance of DICE

**Fig. 1** Basic elements. **a** CE, **b** Clocked CE, **c** ISC, **d** Clocked ISC, **e** TCE



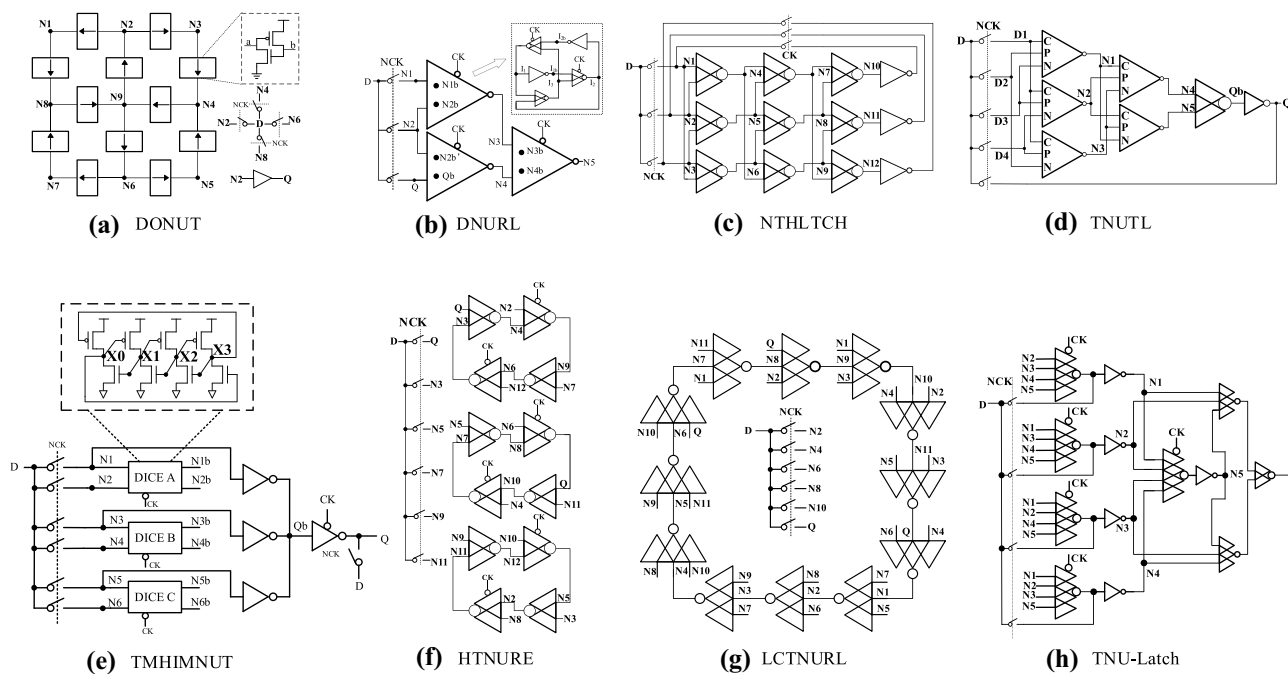


**Fig. 2** Schematics of the previous hardened latches. **a** DONUT, **b** DNURL, **c** NTHLTCH, **d** TNUTL, **e** TMHIMNUT, **f** HTNURE, **g** LCTNURL and **h** TNU-Latch

to realize the tolerance of DNU. DICE consists of 4 cross coupled elements. PMOS and NMOS of the same cross coupled elements are controlled by signals from two different nodes. When the input signal changes, there will be a delay between the control signals of PMOS and NMOS for the same cross coupled element, resulting in short-circuit current and increased circuit power consumption. Similar to DICE, DONUT uses 12 cross coupled elements, which also has short-circuited current and generates short-circuit power consumption. Therefore, the power consumption of DONUT is relatively large. As a one-level buffer is added between input and output, the delay is also large.

DNURL [20] in Fig. 2b is a DNU tolerant latch. Each SNU-Resilient Cell can realize SNU tolerance. DNURL utilizes three SNU-Resilient Cells interconnecting to form a redundant interlocked structure, achieving complete tolerance of DNU. DNURL utilizes a high-speed path, so the delay is small. However, DNURL has more transistors than the proposed DNUL, so the power consumption and area are relatively large.

NTHLTCH [8] in Fig. 2c is a DNU tolerant latch. NTHLTCH utilizes nine C-Elements to constitute 3 × 3 array, filtering the wrong logic value level by level, achieving complete DNU tolerance. NTHLTCH does not use a high-speed path, so the delay is large. NTHLTCH has more transistors than DNUL, so its power consumption is greater than DNUL.

TNUTL [11] in Fig. 2d is a TNU tolerant latch. Based on the blocking ability of the ISC and CE, TNUTL realizes TNU tolerance through three-level filtering of upset. However, there is no feedback loop in TNUTL, so the node logic value is not stable. TNUTL utilizes a high-speed path, and the number of transistors is very small, so the delay and power consumption are very low.

HTNURE [19] in Fig. 2e is a TNU tolerant latch. Based on the tolerance of CE loop to SNU, HTNURE combines three C-Element loops to realize TNU tolerance. HTNURE utilizes a high-speed path and clock-gating, so the delay and power consumption are low. However, HTNURE has 8 more transistors than TNUL.

TMHIMNUT [22] in Fig. 2f is a TNU tolerant latch. Based on the tolerance of DICE to SNU, TMHIMNUT utilizes three DICES and "wired-AND" selector at the output to realize TNU tolerance. TMHIMNUT utilizes a high-speed path, so the delay is low. TMHIMNUT utilizes three DICES, so there is the problem of short-circuit current mentioned above. Therefore, power consumption of TMHIMNUT is high.

LCTNURL [23] in Fig. 2g is a TNU tolerant latch. Based on the powerful blocking ability of Triple-input C-Element, LCTNURL connects 12 Triple-input C-Elements into a loop, and realizes TNU tolerance through the blocking of upset level by level. LCTNURL utilizes high-speed path, so the delay is low. LCTNURL has a large number of transistors

and does not utilize clock-gating, so the power consumption is large.

TNU-Latch [18] in Fig. 2h is a TNU tolerant latch. TNU-Latch utilizes a large number of transistor stacks. Based on the strong blocking ability of clocked quadruple-input C-Element, TNU-Latch attains TNU tolerance. TNU-Latch does not utilize a high-speed path. In the transparent mode, the path from input to output is long, so the delay is very high. The number of TNU-Latch transistors is large, so the power consumption is high.

### 3 Proposed Hardened Latch Design

#### 3.1 Circuit Structure and Working Principles of DNUL

Figure 3 shows the schematic of the proposed DNUL, which consists of four transmission gates (TG<sub>0</sub> ~ TG<sub>3</sub>), six ISCs (ISC<sub>0</sub> ~ ISC<sub>5</sub>) and a TCE. With six internal nodes (N<sub>0</sub> ~ N<sub>5</sub>), the feedback loop of DNUL connects as follows: The In1 (C) of ISC<sub>i</sub> connects to N<sub>i</sub>, In2 (P) connects to N<sub>i+4</sub>, In3 (N) connects to N<sub>i+2</sub>, and output connects to C of ISC<sub>i+1</sub> (i = 0, 1, 2, 3, 4, 5). It should be noted that the numerical operations of subscript are all senary addition operations, represented by "mod6". For example, (3 + 4)<sub>mod6</sub> = 1. D, Q, CK, and NCK are the input, output, clock signal, and complementary clock signal, respectively.

Figure 4 shows the layout of the proposed DNUL design. When CK = 1 and NCK = 0, DNUL works in the transparent mode. TG<sub>0</sub> ~ TG<sub>3</sub> turn on. D propagates to Q only through

one-level transmission gate (TG<sub>3</sub>), which can greatly reduce delay. ISC<sub>1</sub>, ISC<sub>3</sub> and ISC<sub>5</sub> turn off, which can reduce power consumption. D propagates to internal nodes N<sub>0</sub>, N<sub>2</sub> and N<sub>4</sub> through TG<sub>0</sub>, TG<sub>1</sub> and TG<sub>2</sub>, respectively. Then N<sub>1</sub>, N<sub>3</sub> and N<sub>5</sub> are driven by ISC<sub>0</sub>, ISC<sub>2</sub> and ISC<sub>4</sub>, respectively.

When CK = 0 and NCK = 1, DNUL works in the hold mode. TG<sub>0</sub> ~ TG<sub>3</sub> turn off. ISC<sub>1</sub>, ISC<sub>3</sub> and ISC<sub>5</sub> turn on. The signal holds in the feedback loop. The N<sub>1</sub>, N<sub>3</sub>, and N<sub>5</sub> nodes propagate to output Q through TCE.

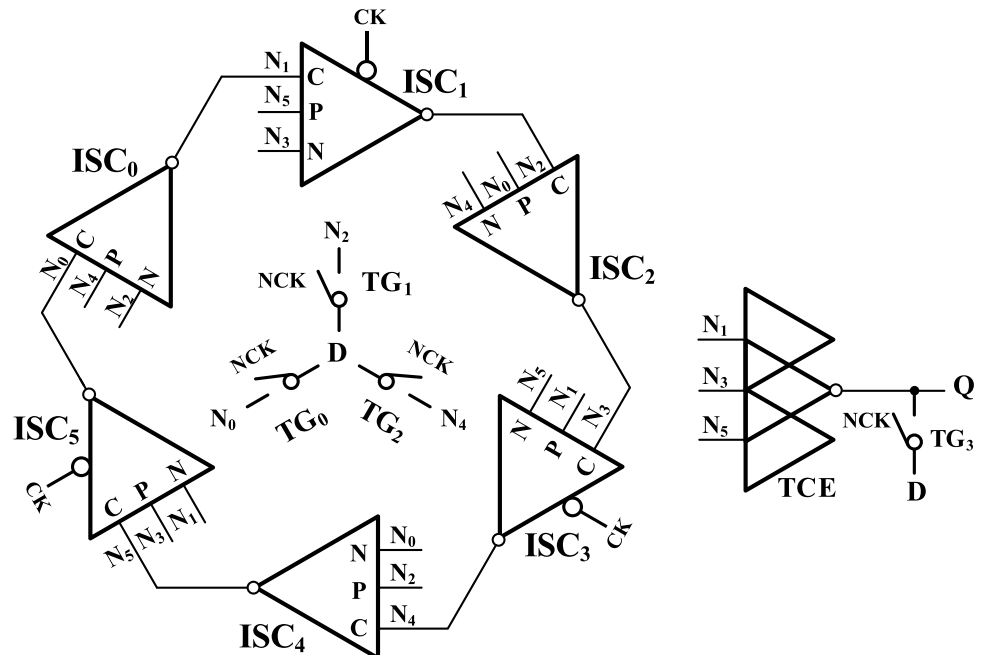
#### 3.2 Fault Tolerance Principle of DNUL

The following is the fault-tolerance analysis of DNUL to SNU and DNU. Before analysis, it is assumed that N<sub>0</sub> = N<sub>2</sub> = N<sub>4</sub> = 0, N<sub>1</sub> = N<sub>3</sub> = N<sub>5</sub> = 1 and Q = 0 in the hold mode. In Figs. 5 and 9, the red lightning symbol in the simulation waveform indicates that a double exponential current source [12] is used to perform fault injection at this position. We adopt the double exponential model for fault injection, and the fault injection node is added with the following current sources:

$$I(t) = \frac{Q}{(\tau_2 - \tau_1)}(e^{-t/\tau_2} - e^{-t/\tau_1}) \tag{1}$$

Compared with the early single exponential current source model, the double exponential current source model can more accurately describe the process of rapid rise and slow decline of leakage current after a particle incident. Therefore, it is suitable and accurate for simulating fault injection. Q is the injected charge of the fault injection node.

Fig. 3 Proposed hardened latch DNUL



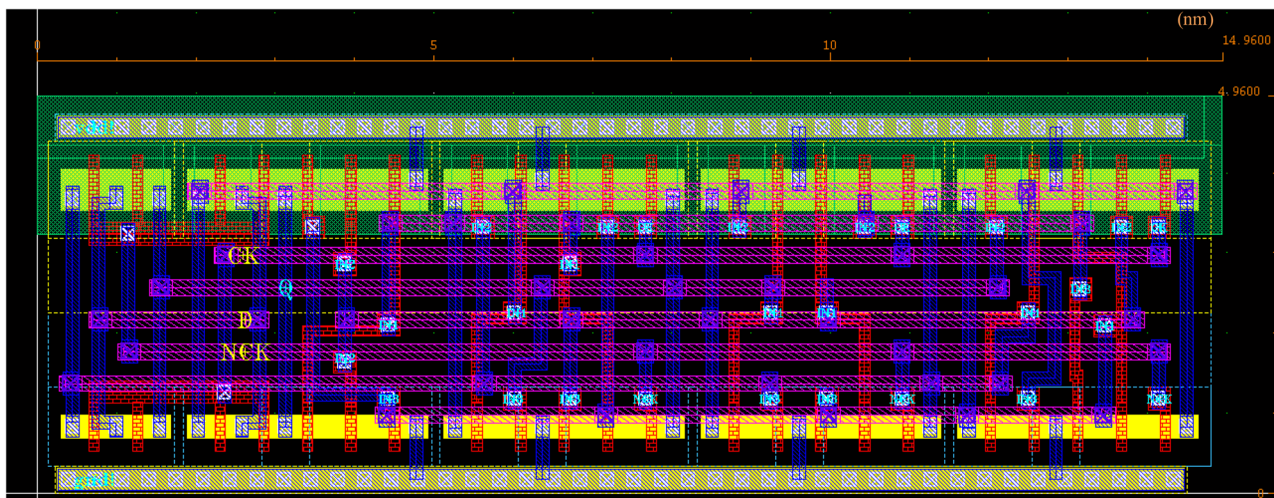


Fig. 4 Layout of the proposed DNUL design

“ $t$ ” is the simulation time for fault injection. “ $\tau_1$ ” is the ion trajectory establishment constant, which is set to 50 ps in the simulation. “ $\tau_2$ ” is the charge accumulation time constant, which is set to 164 ps in the simulation [12, 15, 17].

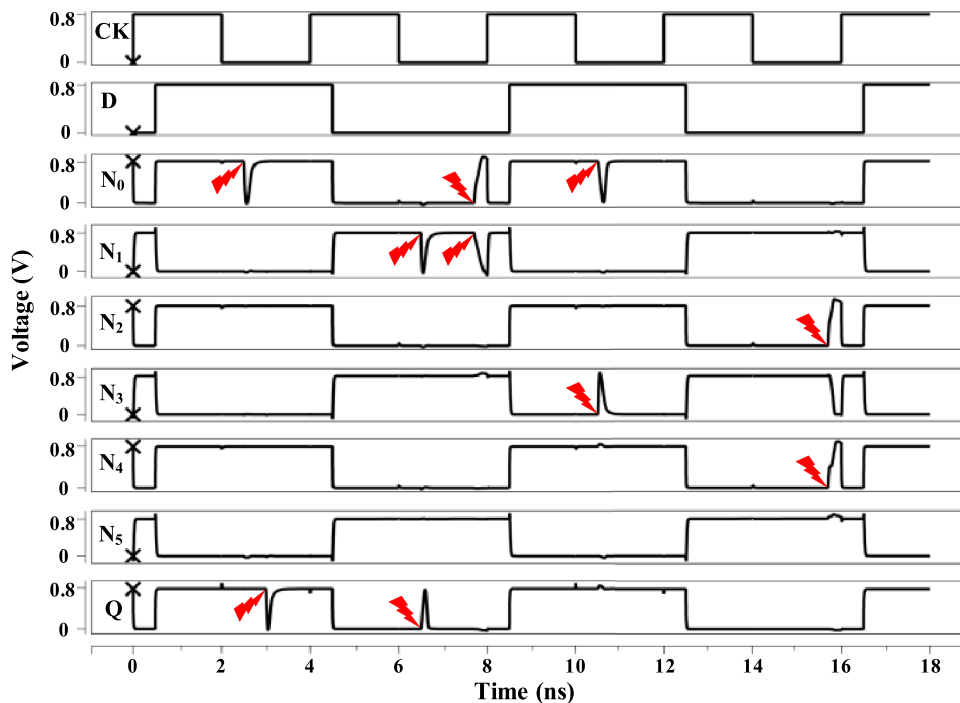
**SNU1** *SNU occurs at an internal node.* Because of the symmetry of DNUL, we can take upset at  $N_0$  as an example. When upset occurs at  $N_0$ , it will not propagate to other internal nodes because of the blocking ability of  $ISC_0$ ,  $ISC_2$  and  $ISC_4$ .  $N_1$ ,  $N_3$  and  $N_5$  quickly recover  $N_0$  to the correct logic

value. As shown in Fig. 5, when fault injection is performed at  $N_0$  at 2.5 ns,  $N_0$  can recover quickly.

**SNU2** *SNU occurs at output node Q.* The internal nodes will not be affected. So  $N_1$ ,  $N_3$  and  $N_5$  quickly recover Q to the correct logic value by TCE. As shown in Fig. 5, fault injection is performed at Q at 3 ns.

DNUL has six internal nodes and one output node. Therefore, there are totally  $C_7^2 = 21$  cases for DNU. We will discuss and classify in three situations.

Fig. 5 Fault injection of DNUL



**DNUL1** *DNU occurs at internal nodes, and the two upset nodes are exactly two inputs of the same ISC.* We discuss the worst case for this situation, such as  $\langle N_2, N_4 \rangle$ .  $N_2$  and  $N_4$  upset from 0 to 1 at the same time. Because of the blocking ability of ISC, the output of  $ISC_0$  and  $ISC_4$  is unchanged. The output of  $ISC_2$  ( $N_3$ ) is upset from 1 to 0. The outputs of both  $ISC_1$  and  $ISC_3$  are in “hold”, so  $N_2$  and  $N_4$  hold the wrong logic value. But  $Q$  does not suffer an upset due to the protection of TCE. Hence, DNUL can completely tolerate the DNU of this situation. Fault injection is performed at  $\langle N_2, N_4 \rangle$  at 15.7 ns in Fig. 5. It can be seen that the latch tolerates this kind of DNU. This situation totals  $2 \times C_3^2 = 6$  cases.

**DNUL2** *DNU occurs at internal nodes, but the two upset nodes are not two inputs of the same ISC.* We discuss the worst case for this situation, such as  $\langle N_0, N_1 \rangle$ .  $N_0$  is upset from 0 to 1 and  $N_1$  is upset from 1 to 0. Therefore, the outputs of both  $ISC_0$  and  $ISC_5$  are in “hold”, i.e.,  $N_0$  and  $N_1$  cannot recover to the correct logic values. But other internal nodes are not affected, so  $Q$  holds the correct logic value because of the filtering of TCE. Hence, DNUL can completely tolerate the DNU of this situation. As shown in Fig. 5, the fault injections are performed at  $\langle N_0, N_1 \rangle$  and  $\langle N_0, N_3 \rangle$  at 7.6 ns and 10.5 ns, respectively. It can be seen that the latch tolerates this kind of DNU. This situation totals  $C_3^1 \times C_3^1 = 9$  cases.

**DNUL3** *DNU occurs at one internal node and the output Q at the same time.* Taking  $\langle N_1, Q \rangle$  as an example, after  $N_1$  is upset, it recovers to the correct logic value by  $ISC_0$ .  $Q$  also recovers to the correct logic value by TCE. Hence, DNUL can achieve complete tolerance and also self-recovery to the DNU of this situation. Fault injection is performed at  $\langle N_1, Q \rangle$  at 6.5 ns in Fig. 5. It can be seen that the latch tolerates this kind of DNU. This situation totals  $C_6^1 = 6$  cases.

In summary, three situations of DNU contain  $6 + 9 + 6 = 21$  sub-cases, i.e., it covers all DNU cases. The above proves that DNUL can completely tolerate DNU. DNUL is a blocking latch. When the data is stored for a long time and DNU occurs, the output may be in the high impedance state. There will be leakage current which makes the logic value unstable. In order to ensure the correct output logic value, we can add a keeper to the output to drive the output. DNUL\_keeper is shown in Fig. 6. For very low-frequency applications, we can use DNUL\_keeper. For current mainstream chips, the operating frequency is generally hundreds of megahertz so that DNUL can be fully competent.

### 3.3 Circuit Structure and Working Principles of TNUL

Figure 7 shows the schematics of TNUL. Compared to DNUL, the feedback loop of TNUL adds two ISCs. The

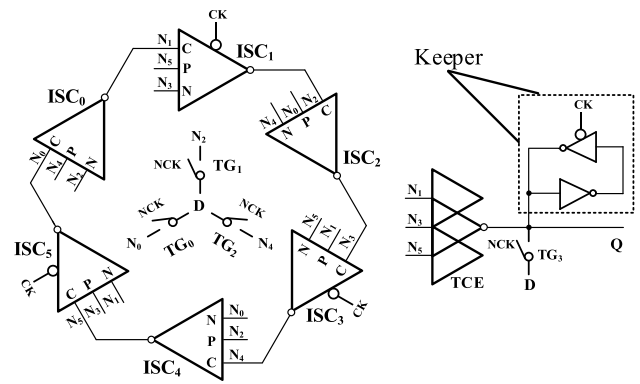


Fig. 6 The schematic of the DNUL\_keeper

number of internal nodes also increases to eight ( $N_0 \sim N_7$ ). To tolerate TNU, the output level of TNUL uses two-level CEs ( $C_0, C_1$  and  $C_2$ ). The output level nodes include  $X_0, X_1$  and  $Q$ .

Figure 8 shows the layout of the proposed DNUL design. The feedback loop of TNUL connects in this way: The In1 (C) of  $ISC_i$  connects to node  $N_i$ , In2 (P) connects to  $N_{i+6}$ , In3 (N) connects to  $N_{i+4}$ , and output connects to C of  $ISC_{i+1}$  ( $i = 0, 1, 2, 3, 4, 5, 6, 7$ ). Similarly, the numerical operations of subscript are all octonary addition operations, represented by “mod8”. TNUL works the same way as DNUL whether in the transparent mode or hold mode, so no additional analysis is performed.

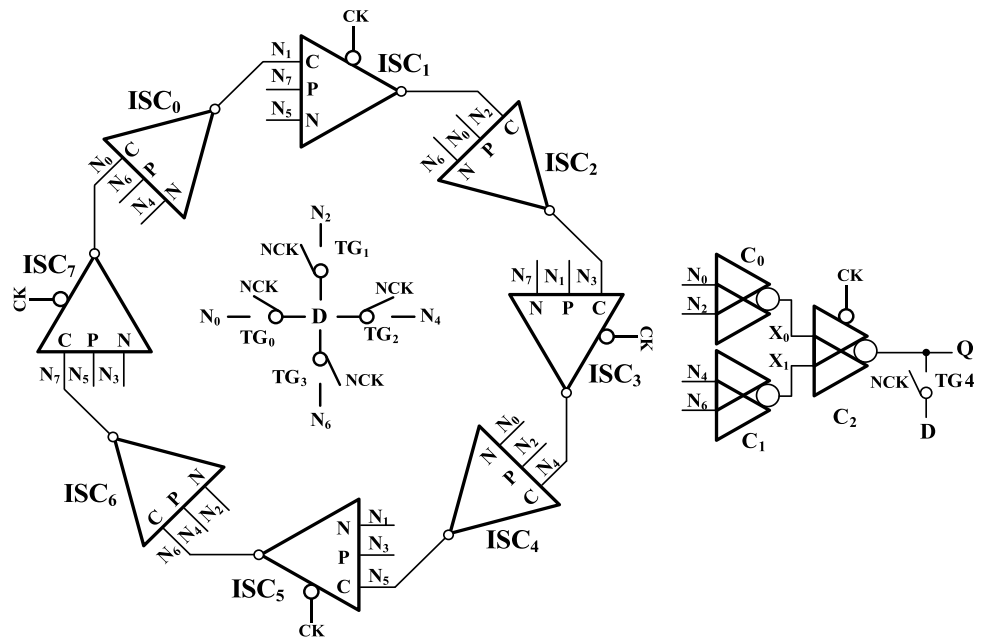
### 3.4 Fault Tolerance Principle of TNUL

Since the fault tolerance principle of TNUL to SNU and DNU is the same as DNUL, we no longer analyze them. Figure 9 shows the fault injection of SNU and DNU: At  $N_2$  at 2.5 ns; At  $X_0$  at 3 ns; At  $Q$  at 3.5 ns; At  $\langle N_0, N_1 \rangle$  at 6.5 ns; At  $\langle N_0, Q \rangle$  at 10.5 ns.

There are  $C_{11}^3 = 165$  TNU cases, which are classified into the following four situations for analysis:

**TNU1** *TNU only occurs at the feedback loop.* The worst cases of this situation can result in some nodes not recovering to the correct logic value. Taking  $\langle N_0, N_2, N_3 \rangle$  as an example,  $N_0$  and  $N_2$  are upset from 0 to 1, and  $N_3$  is upset from 1 to 0.  $X_0$  suffers an upset from 1 to 0 by  $C_0$ . Therefore, the outputs of both  $ISC_2$  and  $ISC_7$  are in “hold”, so  $N_3$  and  $N_0$  hold the wrong logic value.  $X_0$  also holds the wrong logical value by  $C_0$ . But under the filtering of the CEs of the output level,  $Q$  is not affected. Anyway, TNUL can completely tolerate TNU in this situation. As shown in Fig. 9, the fault injection is performed at  $\langle N_0, N_2, N_3 \rangle$  and  $\langle N_1, N_3, N_5 \rangle$  at 7.7 ns and 11.5 ns, respectively. It can be seen that the latch tolerates this kind of TNU. This situation totals  $C_8^3 = 56$  cases.

**Fig. 7** Proposed hardened latch TNUL



**TNU2** Two upset nodes are at the feedback loop and one upset node is at the output level. Discussing the worst case, i.e.,  $\langle N_1, N_6, X_1 \rangle$ ,  $N_1$  and  $X_1$  are upset from 1 to 0, and  $N_6$  is upset from 0 to 1. Therefore, the outputs of both  $ISC_0$  and  $ISC_5$  are in “hold”, so  $N_1$  and  $N_6$  hold the wrong logic value.  $X_1$  also holds the wrong logical value by  $C_1$ . But under the filtering of the  $C_2$  of the output level,  $Q$  is not affected. In a word, TNUL can completely tolerate TNU in this situation. As shown in Fig. 9, the fault injection is performed at  $\langle N_1, N_6, X_1 \rangle$  at 15.5 ns. It can be seen that the latch tolerates this kind of TNU. This situation totals  $C_8^2 \times C_3^1 = 84$  cases.

**TNU3** One upset node is at the feedback loop and two upset nodes are at the output level. Known from the above analysis, single node upset at the feedback loop can achieve

self-recovery, and then refresh the logic value of the output level nodes to achieve TNU self-recovery of this situation. As shown in Fig. 9, fault injection is performed at  $\langle N_0, X_0, Q \rangle$  at 18.5 ns. It can be seen that the latch tolerates this kind of TNU. This situation totals  $C_8^1 \times C_3^2 = 24$  cases.

**TNU4** TNU only occurs at the output level, i.e.,  $X_0, X_1$  and  $Q$  upset at the same time. The nodes at the feedback loop will not be affected. So  $X_0, X_1$  and  $Q$  quickly recover to the correct logic value by  $C_0, C_1$  and  $C_2$ , respectively. As shown in Fig. 9, fault injection is performed at  $\langle X_0, X_1, Q \rangle$  at 19.5 ns. This situation totals one case.

Four situations contain  $56 + 84 + 24 + 1 = 165$  sub-cases, i.e., it covers all TNU cases. The above proves that TNUL is completely tolerant to TNU. Like DNUL\_keeper,

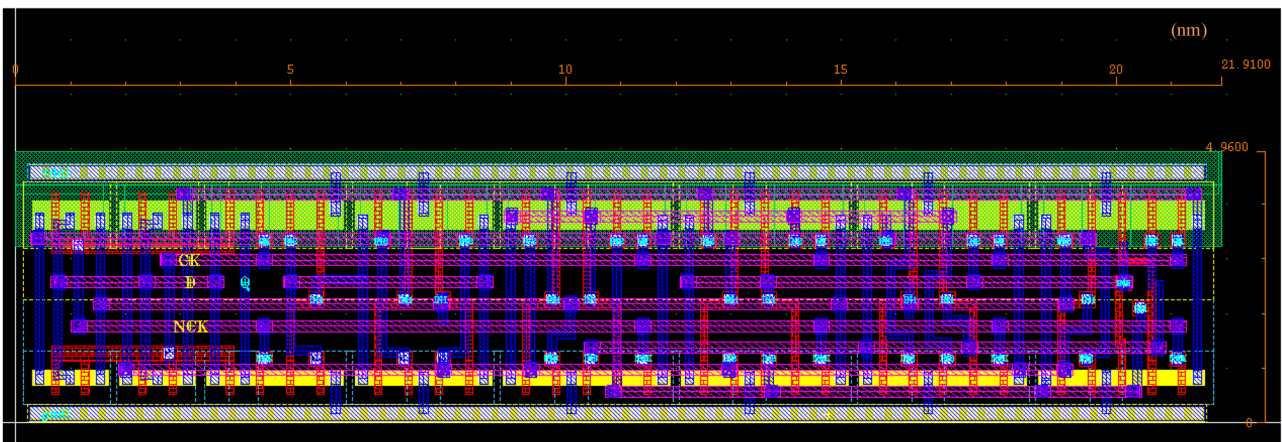
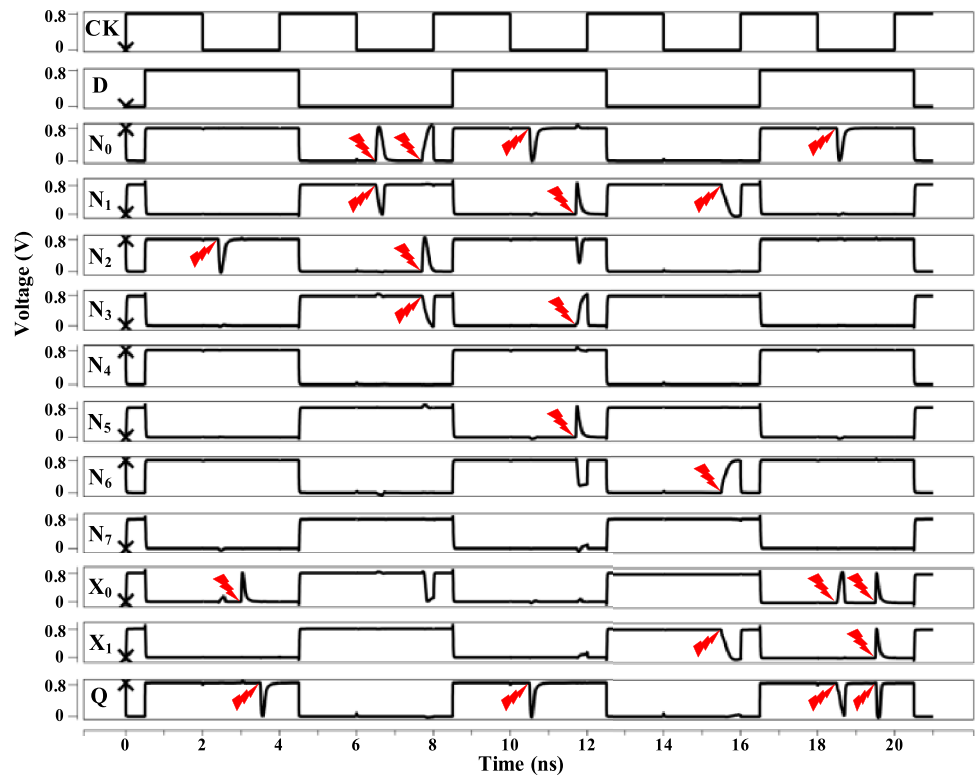


**Fig. 8** Layout of the proposed TNUL design

Fig. 9 Fault injection of TNUL



TNUL can also add keeper to the output to keep the output logic is correct. For mainstream applications, TNUL is fully competent.

## 4 Evaluation and Comparison

This part evaluates and compares the proposed latches with previous hardened latches, in terms of hardened performance, overhead and sensitivity to variation.

### 4.1 The Comparison of Hardened Performance and Overhead

To ensure fairness, the simulation conditions are the same for the proposed latches and the compared latches. The simulation software used is HSPICE. Simulation conditions are set as 22 nm CMOS process, 0.8 V supply voltage, 25 °C temperature and 250 MHz clock frequency.

Under the premise of ensuring that the circuit can work properly, the PMOS transistor has  $W/L = 88/22$  nm while the NMOS transistor has  $W/L = 44/22$  nm. Table 1 shows the comparison in terms of hardened performance and overhead. The second to fourth columns represent the hardened performance, which indicates whether the SNU, DNU and TNU are fully tolerated, respectively. “√” means that the

latch can tolerate, “×” means that the latch cannot tolerate. It can be seen from Table 1 that the comparison latches DONUT, DNURL, NTHLTC and the proposed DNUL can tolerate SNU and DNU; the comparison latches TNUTL, HTNURE, TMHIMNUT, LCTNURL, TNU-Latch and the proposed TNUL can fully tolerate SNU, DNU and TNU. The following is the comparison of the critical charge of each latch, and  $Q_{crit}$  is the critical charge. For fairness of comparison, the critical charge is the injected charge when the node happens to have full swing. For DNU tolerant latch,  $Q_{crit}$  represents the minimum charge required to upset the two internal nodes at the same time; For TNU tolerant latch,  $Q_{crit}$  represents the minimum charge required to upset the three internal nodes at the same time. However, these upsets will be tolerated by the hardening latch, and the output of the latch will not be affected.

The Delay refers to the propagation delay, that is, the D-Q delay. Power denotes the average power consumption of the latch within 20 ns [16]. The Area designation corresponds to the silicon area extracted from layout comparisons.  $T_{setup}$  is the setup time. For the input of the latches,  $T_{setup}$  is the minimum setup time before the CLK high level disappears.  $T_{setup}$  is equivalent to the time required to establish stable logic values for all internal nodes and output Q in transparent mode [8]. The smaller the setup time, the faster the latch responds to the input change, which means the better the latch performance.



**Table 1** Comparison of performance and overhead of latches

Latch	SNU	DNU	TNU	$Q_{crit} / fC$	Delay / ps	Power / $\mu w$	PDP / aJ	$10^{-3} \times \text{Area} / \mu m^2$	$T_{setup} / ps$
DONUT [4]	✓	✓	×	5.45	24.06	1.19	28.63	60.70	28.12
DNURL [20]	✓	✓	×	3.76	3.02	0.92	2.78	111.29	59.05
NTHLTCH [8]	✓	✓	×	4.42	12.39	0.76	9.42	97.81	62.63
DNUL (proposed)	✓	✓	×	4.05	2.30	0.28	0.64	74.20	22.03
TNUTL [11]	✓	✓	✓	1.68	7.42	0.32	2.37	63.24	47.79
HTNURE [19]	✓	✓	✓	3.93	2.88	0.44	1.27	126.49	19.23
TMHIMNUT [22]	✓	✓	✓	3.98	1.54	0.84	1.29	112.44	7.96
LCTNURL [23]	✓	✓	✓	3.50	4.84	0.83	4.02	147.58	57.69
TNU-Latch [18]	✓	✓	✓	6.45	92.61	0.85	78.72	144.06	95.32
TNUL (proposed)	✓	✓	✓	4.50	1.52	0.39	0.59	108.92	21.07

In order to compare the latch performance comprehensively, we introduce PDP. Formula (2) shows the calculation of PDP.

$$PDP = Delay \times Power \quad (2)$$

Compared with the latches with the same hardened performance (DONUT, DNURL and NTHLTCH), the delay, power consumption, PDP and the setup time of the DNUL are optimal, the area overhead of DNUL is suboptimal. The delay and PDP of TNUL are optimal in the comparison with all compared latches. Compared with the latches with the same hardened performance (TNUTL, HTNURE, TMHIMNUT, LCTNURL and TNU-Latch), the delay and PDP of the TNUL are optimal, and the critical charge, power consumption and area overhead are suboptimal. The proposed TNUL is better than TNUTL, LCTNURL and TNU-Latch, and worse than HTNURE and TMHIMNUT in terms of the setup time.

## 4.2 PVT Variation Analysis

With advances in IC process, latches become more sensitive to variations of PVT [1]. Based on the stable working characteristics of ISC and CE, the proposed latches are insensitive to variations of PVT. As shown in Figs. 10 and 11, for comparing the stability of each latch, variation analysis is performed for the proposed latches as well as for the DNU and TNU tolerant latches.

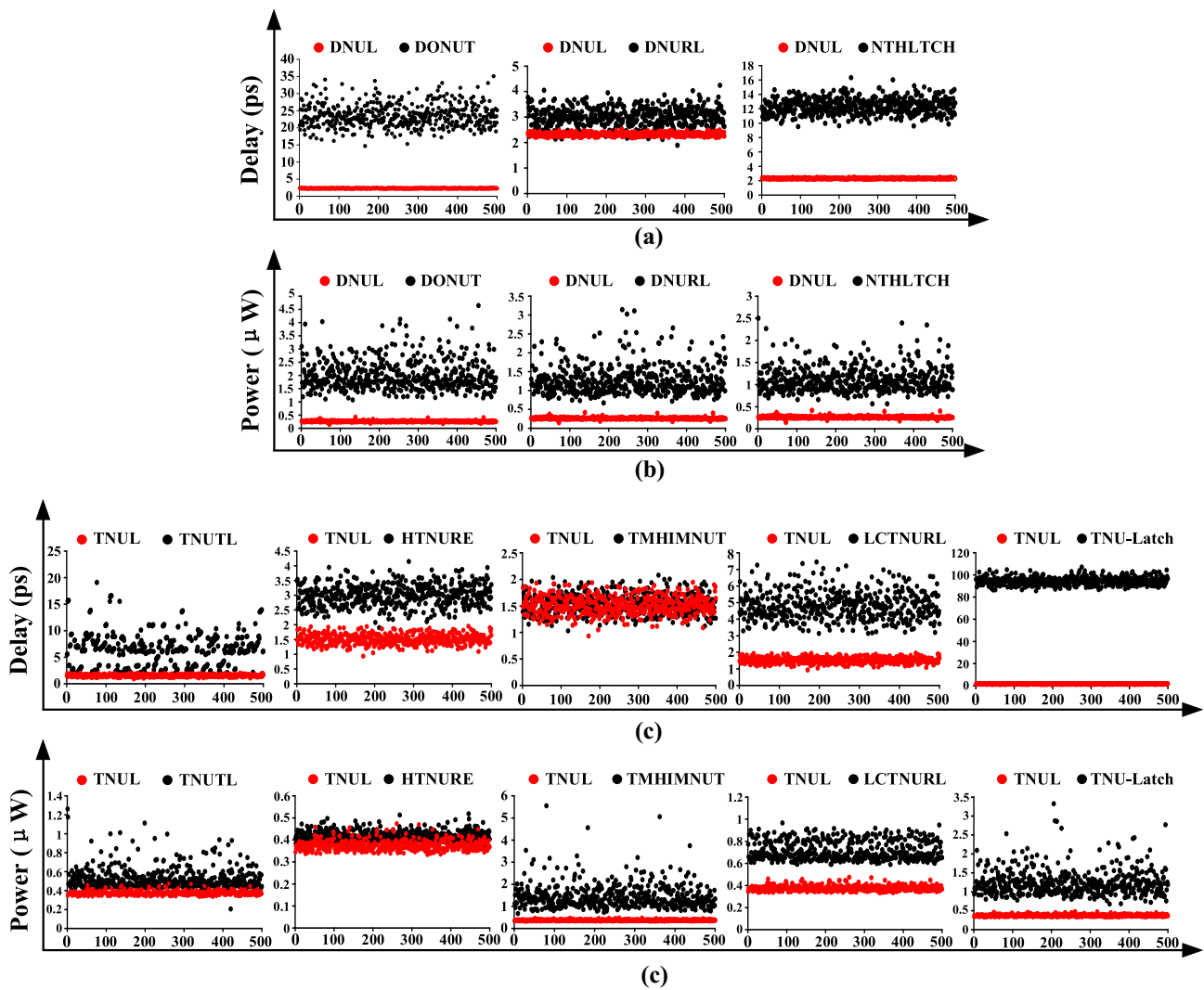
As shown in Fig. 10, Monte Carlo simulations based on 500 samples were performed by sweeping the gate length using a  $\pm 10\%$  Gaussian distribution with variation at the  $\pm 3\sigma$  level and the gate oxide using a  $\pm 10\%$  Gaussian distribution with variation at the  $\pm 3\sigma$  level. Figure 10a is the comparison scatter diagram of delay variation between the proposed DNUL and the DNU tolerant latches after Monte Carlo simulation; Fig. 10b is the comparison scatter

diagram of power consumption variation between DNUL and the DNU tolerant latches after Monte Carlo simulation; Fig. 10c is the comparison scatter diagram of delay variation between TNUL and the TNU tolerant latches after Monte Carlo simulation; Fig. 10d is the comparison scatter diagram of power consumption between the proposed TNUL and the TNU tolerant latches after Monte Carlo simulation. The abscissa represents 500 simulation times. In order to facilitate the observation of data variation, the comparison diagrams of the proposed latches and the comparison latches are displayed independently.

Figure 10a shows the variation of the delay of the DNU tolerant latches with the variation of process. Figure 10b shows the variation of the power consumption of the DNU tolerant latches with the variation of process. Figure 10c shows the variation of the delay of the TNU tolerant latches with the variation of process. Figure 10d shows the variation of the power consumption of the TNU tolerant latches with the variation of process. The scatter plots of the proposed latches are very concentrated. The more concentrated the scatter distribution, the lower the sensitivity of the latch to process variations. The results show that the proposed latches have very low sensitivity to process variation.

Figure 11 is the voltage and temperature variation analysis. Figure 11a shows the variation of delay at different voltages; Fig. 11b shows the variation of power consumption at different voltages; Fig. 11c shows the variation of delay at different temperatures; Fig. 11d shows the variation of power consumption at different temperatures. In Fig. 11a and c, because of the large delay of TNU-Latch, the delay of TNU-Latch uses the right longitudinal axis, and the other latches use the left longitudinal axis. As we can see from Fig. 11, the variations of delay and power consumption of DNUL and TNUL are low.

These validate the high stability of the proposed DNUL and TNUL.



**Fig. 10** Monte Carlo simulations. **a** The variation of delay of the DNU tolerant latches with the variation of process, **b** The variation of power consumption of the DNU tolerant latches with the variation

of process, **c** The variation of delay of the TNU tolerant latches with the variation of process, **d** The variation of power consumption of the TNU tolerant latches with the variation of process

### 5 Conclusion

For the increasing problems of DNU and TNU, this paper proposes DNUL and TNUL, respectively. Based on the robust blocking property of the ISC, we use a subtle interconnection way and connect the ISCs into a large feedback loop to maintain the logic value. Then, the CEs at the output level filter the wrong logic value, so that DNUL and

TNUL can effectively tolerate DNU and TNU, respectively. Through the introduction of clock-gating and high-speed path technique, DNUL and TNUL attain very low overhead. At the same time, Monte Carlo simulations and Voltage and Temperature Variation analysis show that the proposed latches are insensitive to variations of PVT and have high stability.

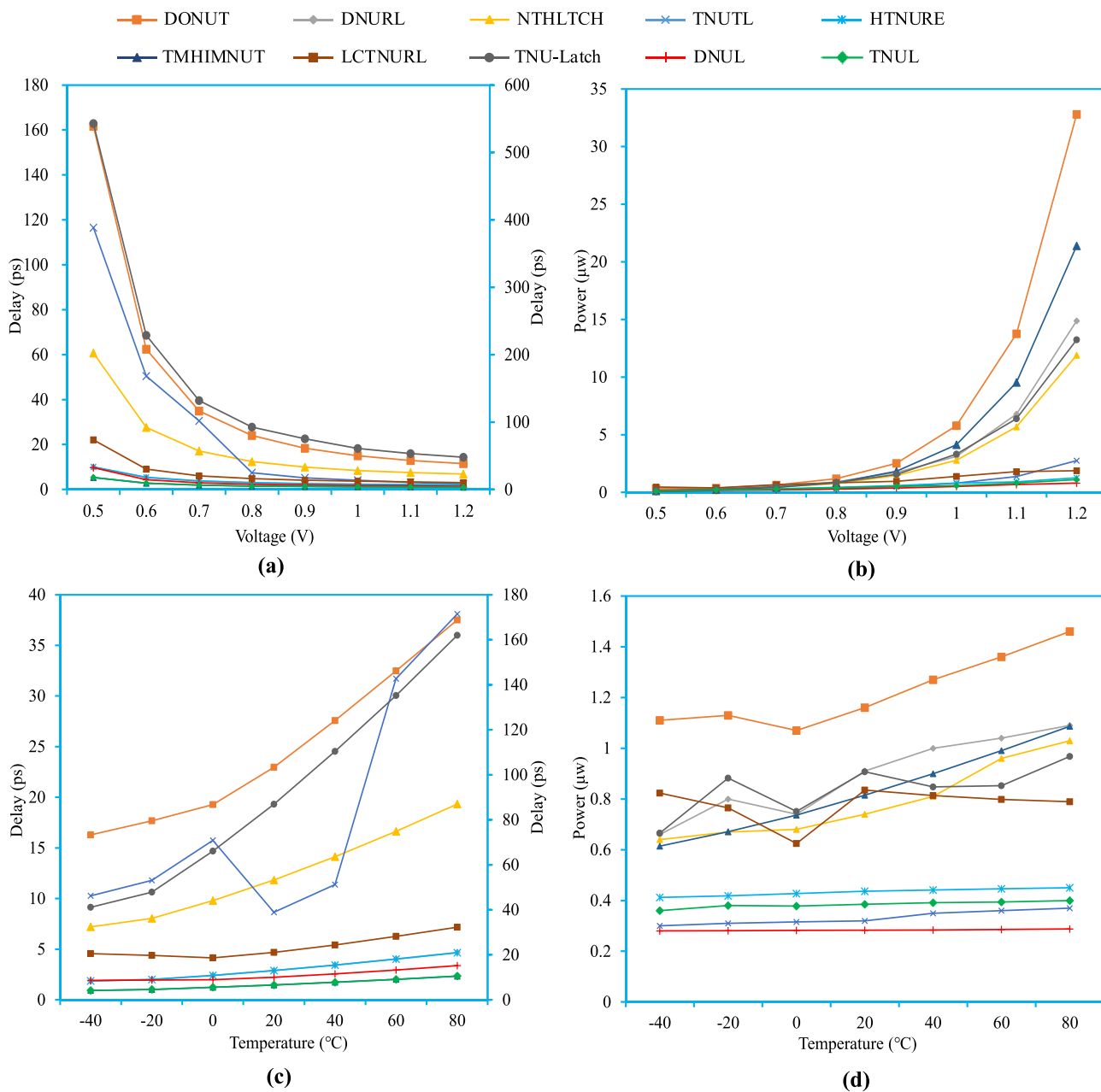


**Fig. 11** Voltage and Temperature Variations analysis. **a** The variation of delay at different voltages, **b** The variation of power consumption at different voltages, **c** The variation of delay at different temperatures, **d** The variation of power consumption at different temperatures

**Funding** This work was supported in part by National Natural Science Foundation of China under grant nos. 62274052, 61834006, 62027815, 61874157.

**Data Availability** The datasets generated and analyzed during the current study are available from the corresponding author on reasonable request.

**Declarations**

**Conflicts of Interests** The authors declare that they have no known competing financial interests or personal relationships that could have appeared to influence the work reported in this paper.

## References

- Alioto M, Consoli E, Palumbo G (2015) Variations in Nanometer CMOS flip-flops: part II – energy variability and impact of other sources of variations. *IEEE Trans Circuits Syst I Regul Pap* 62(3):835–843. <https://doi.org/10.1109/TCSI.2014.2366813>
- Calin T, Nicolaidis M, Velazco R (1996) Upset hardened memory design for submicron CMOS technology. *IEEE Trans Nucl Sci* 43(6):2874–2878. <https://doi.org/10.1109/23.556880>
- Ebara M, Yamada K, Kojima K, Furuta J, Kobayashi K (2019) Process dependence of soft errors induced by alpha particles, heavy ions, and high energy neutrons on flip flops in FDSOI. *IEEE J Electron Devices Soc* 7:817–824. <https://doi.org/10.1109/JEDS.2019.2907299>
- Eftaxiopoulos N, Axelos N, Pekmestzi K (2015) DONUT: a double node upset tolerant latch. 2015 IEEE Computer Society Annual Symposium on VLSI, pp 509–514. <https://doi.org/10.1109/ISVLSI.2015.72>
- Fazeli M, Patooghy A, Miremadi SG, Ejlali A (2007) Feedback redundancy: a power efficient SEU-tolerant latch design for deep sub-micron technologies. *IEEE/IFIP International Conference on Dependable Systems and Networks (DSN'07)*, pp 276–285. <https://doi.org/10.1109/DSN.2007.51>
- Ferlet-Cavrois V, Massengill LW, Gouker P (2013) Single event transients in digital CMOS – a review. *IEEE Trans Nucl Sci* 60(3):1767–1790. <https://doi.org/10.1109/TNS.2013.2255624>
- Ibe E, Taniguchi H, Yahagi Y, Shimbo K, Toba T (2010) Impact of scaling on neutron-induced soft error in SRAMs from a 250 nm to a 22 nm design rule. *IEEE Trans Electron Devices* 57(7):1527–1538. <https://doi.org/10.1109/TED.2010.2047907>
- Li Y, Wang H, Yao S, Yan X, Gao Z, Xu J (2015) Double node upsets hardened latch circuits. *J Electron Test* 31(5):537–548. <https://doi.org/10.1007/s10836-015-5551-3>
- Liang H, Li X, Huang Z, Yan A, Xu X (2017) Highly robust double node upset resilient hardened latch design. *IEICE Trans Electron* E100(5):496–503. <https://doi.org/10.1587/transele.E100.C.496>
- Lin S, Kim Y, Lombardi F (2012) Analysis and design of nanoscale CMOS storage elements for single-event hardening with multiple-node upset. *IEEE Trans Device Mater Reliab* 12(1):68–77. <https://doi.org/10.1109/TDMR.2011.2167233>
- Liu X (2019) Multiple node upset-tolerant latch design. *IEEE Trans Device Mater Reliab* 19(2):387–392. <https://doi.org/10.1109/TDMR.2019.2912811>
- Messenger GC (1982) Collection of charge on junction nodes from ion tracks. *IEEE Trans Nucl Sci* 29(6):2024–2031. <https://doi.org/10.1109/TNS.1982.4336490>
- Mitra S, Seifert N, Zhang M, Shi Q, Kim KS (2005) Robust system design with built-in soft-error resilience. *Computer* 38(2):43–52. <https://doi.org/10.1109/mc.2005.70>
- Nan H, Choi K (2012) High performance, low cost, and robust soft error tolerant latch designs for nanoscale CMOS technology. *IEEE Trans Circuits Syst I Regul Pap* 59(7):1445–1457. <https://doi.org/10.1109/TCSI.2011.2177135>
- Neale A, Sachdev M (2016) Neutron radiation induced soft error rates for an adjacent-ECC protected SRAM in 28 nm CMOS. *IEEE Trans Nucl Sci* 63(3):1912–1917. <https://doi.org/10.1109/TNS.2016.2547963>
- Neil Weste HE, Harris DM (2011) *CMOS VLSI design: a circuits and systems perspective*, 4th edn. Addison-Wesley, Boston, MA, USA, p 318 (Proc.)
- Omana M, Rossi D, Metra C (2007) Latch susceptibility to transient faults and new hardening approach. *IEEE Trans Comput* 56(9):1255–1268. <https://doi.org/10.1109/TC.2007.1070>
- Watkins A, Tragoudas S (2020) Radiation hardened latch designs for double and triple node upsets. *IEEE Trans Emerging Top Comput* 8(3):616–626. <https://doi.org/10.1109/TETC.2017.2776285>
- Xu H, Sun C, Zhou L, Liang H, Huang Z (2021) Design of a highly robust triple-node-upset self-recoverable latch. *IEEE Access* 9:113622–113630. <https://doi.org/10.1109/ACCESS.2021.3104335>
- Yan A, Huang Z, Yi M, Xu X, Ouyang Y, Liang H (2017) Double-node-upset-resilient latch design for nanoscale CMOS technology. *IEEE Trans Very Large Scale Integr VLSI Syst* 25(6):1978–1982. <https://doi.org/10.1109/TVLSI.2017.2655079>
- Yan A, Lai C, Zhang Y, Cui J, Huang Z, Song J, Guo J, Wen X (2018) Novel low cost, double and-triple-node-upset-tolerant latch designs for nano-scale CMOS. *IEEE Trans Emerging Top Comput* 99:1–14. <https://doi.org/10.1109/TETC.2018.2871861>
- Yan A, Xu Z, Yang K, Cui J, Huang Z, Girard P, Wen X (2020) A novel low-cost TMR-without-voter based HIS-insensitive and MNU-tolerant latch design for aerospace applications. *IEEE Trans Aerosp Electron Syst* 56(4):2666–2676. <https://doi.org/10.1109/TAES.2019.2951186>
- Yan A, Hu Y, Cui J, Chen Z, Huang Z, Ni T, Girard P, Wen X (2020) Information assurance through redundant design: a novel TNU error-resilient latch for harsh radiation environment. *IEEE Trans Comput* 69(6):789–799. <https://doi.org/10.1109/TC.2020.2966200>
- Zhu X, Deng X, Baumann R, Krishnan S (2007) A quantitative assessment of charge collection efficiency of N+ and P+ diffusion areas in terrestrial neutron environment. *IEEE Trans Nucl Sci* 54(6):2156–2161. <https://doi.org/10.1109/TNS.2007.908758>

**Publisher's Note** Springer Nature remains neutral with regard to jurisdictional claims in published maps and institutional affiliations.

Springer Nature or its licensor (e.g. a society or other partner) holds exclusive rights to this article under a publishing agreement with the author(s) or other rightsholder(s); author self-archiving of the accepted manuscript version of this article is solely governed by the terms of such publishing agreement and applicable law.

**Zhengfeng Huang** received the Ph.D. degree in computer engineering from Hefei University of Technology in 2009. He is a full professor since 2018. His current research interests include design for soft error tolerance/mitigation. He is a member of Technical Committee on Fault Tolerant Computing which belongs to China Computer Federation. He worked as a visiting scholar at the University of Paderborn, Germany from 2014 to 2015. He served on the organizing committee of the IEEE European Test Symposium in 2014. He served as a program cochair of Asian Test Symposium in 2018.

**Hao Wang** is currently working toward the M.S. degree in electronic information in Hefei University of Technology, Hefei, China. His research interests include soft error rate analysis of digital IC and radiation hardening for latches.

**Dongxing Ma** is currently working toward the M.S. degree in electronic information in Hefei University of Technology, Hefei, China. His research interests include soft error rate analysis of digital IC and radiation hardening for latches.

**Huaguo Liang** was born in 1959. He received the Ph.D. degree in computer science from the University of Stuttgart, Germany, in 2003. From 1998 to 2003, he worked as a Research Fellow with the Department of Computer Science, University of Stuttgart. He is currently a Professor and a Ph.D. Supervisor with the Schools of both Computer and Information, and Electronic Science and Applied Physics, HFUT, Hefei, China, where he is also the Dean with the School of Electronic Science and Applied Physics, and the School of Microelectronics. He has directed many projects (e.g., DFG, National Natural Science Foundation, Scientific Research Foundation for the Returned Overseas Chinese Scholars, and State Education Ministry). He has published a book in Germany and more than 100 journal articles. His research interests include built-in-self-test, design automation of digital systems, ATPG algorithms, and distributed control. He served as the General Chair in the organizing committee of the IEEE Asian Test Symposium in 2018.

**Yiming Ouyang** received the bachelor's, master's, and doctoral degrees from Hefei University of Technology in 1984, 1991, and 2013, respectively. He is currently a professor at Hefei University of Technology and a leading expert in research. His main research directions are NoC and on-Chip Systems (SoC), integration and testing of embedded systems, and automation of digital system design.

**Aibin Yan** received the Ph.D. degree in Computer Application Technology from Hefei University of Technology, and received the M.S. degree in Software Engineering from the University of Science and Technology of China (USTC), Hefei, in 2015 and 2009, respectively. In 2016, he joined Anhui University, and currently he is an associate professor. His research interests mainly include radiation hardening for CMOS ICs such as latches, flipflops, and memory cells.